AGE ESTIMATE OF NOVEL WHITE DWARF OPEN CLUSTER WITH ABNORMAL PROPER MOTIONS

An Undergraduate Research Scholars Thesis

by

WILL CHISHOLM[1]

Submitted to the LAUNCH: Undergraduate Research office at
Texas A&M University
in partial fulfillment of the requirements for the designation as an

UNDERGRADUATE RESEARCH SCHOLAR

Approved by
Faculty Research Advisor: Louis Strigari

May 2022

Major: Physics[1]

RESEARCH COMPLIANCE CERTIFICATION

Research activities involving the use of human subjects, vertebrate animals, and/or biohazards must be reviewed and approved by the appropriate Texas A&M University regulatory research committee (i.e., IRB, IACUC, IBC) before the activity can commence. This requirement applies to activities conducted at Texas A&M and to activities conducted at non-Texas A&M facilities or institutions. In both cases, students are responsible for working with the relevant Texas A&M research compliance program to ensure and document that all Texas A&M compliance obligations are met before the study begins.

I, Will Chisholm[1], certify that all research compliance requirements related to this Undergraduate Research Scholars thesis have been addressed with my Research Faculty Advisor prior to the collection of any data used in this final thesis submission.

This project did not require approval from the Texas A&M University Research Compliance & Biosafety office.

TABLE OF CONTENTS

ABSTRACT

[Age Estimate of Novel White Dwarf Open Cluster with Abnormal Proper Motions]

Will Chisholm[1]
Department of Physics and Astronomy[1]
Texas A&M University

Research Faculty Advisor: Louis Strigari
Department of Physics and Astronomy
Texas A&M University

White dwarf open clusters can provide significant insight into the Milky Way local spiral structure as ancient tracers. We analyze a sample of 20 high-confidence white dwarfs from *Gaia EDR3*$\times$*DES Y6 Gold Release* with abnormal proper motions and positioning in color space. We make use of previously derived stellar parameters and theoretical white dwarf cooling sequences to estimate cooling ages for this sample, and by extension a potential new open cluster. We present 11 of the objects as candidate open cluster members, and estimate a cluster cooling age of $\tau = 2.2(1.0)$ Gyr. We finally discuss ways to reduce age estimate uncertainties and how these findings can be used to further probe the local spiral structure.

ACKNOWLEDGMENTS

Contributors

I would like to thank my faculty advisor, Dr. Louis Strigari, as well as the other members of the Milky Way Astronomy group at Texas A&M University, including Dr. Jennifer Marshall, Paul Zivick, Addy Evans, and others for their guidance and support throughout the course of this research.

Thanks also go to my friends and colleagues, including Erica Quist, Agam Shayit, Manu Samala, Krista Anderson, Calista Resse, Vanessa Niccum, and the department faculty and staff for their love and support.

The astronomical data analyzed/used for *Age estimate of novel white dwarf open cluster with abnormal proper motions* were provided by the Gaia Collaboration and European Space Agency [1], as well as the Dark Energy Survey Team and National Science Foundation [2].

All other work conducted for the thesis was completed by the student independently.

Funding Sources

Undergraduate research was supported by the *Department of Physics and Astronomy Summer Undergraduate Research Stipend* at Texas A&M University.

NOMENCLATURE

Gaia	Gaia Survey, described in [1]
DES	Dark Energy Survey, described in [2]
SDSS	The Sloan Digital Sky Survey, described in [3]
ADQL	Astronomical Data Query Language (similar to SQL)
α	Right Ascension (longitudinal coordinate)
δ	Declination (latitudinal coordinate)
ϖ	Parallax
μ_α	Angular change in right ascension for a given length of time
$\mu_{\alpha*}$	Proper Motion in right ascension, that is $\mu_{\alpha*} = \mu_\alpha \cos\delta$
μ_δ	Proper Motion in declination
μ	Total proper motion, that is $\mu^2 = \mu_{\alpha*}^2 + \mu_\delta^2$
$\mu_{\alpha*}$	Proper Motion in right ascension
σ_x	The uncertainty of the measurement of x
G	Absolute magnitude in the G-bandpass filter (also applies to other bandpass filters such as R, I, Z, etc ...)
g	Apparent magnitude in the G-bandpass filter (also applies to other bandpass filters such as r, i, z, etc ...)
$g - r$	$g - r$ color of object
T_{eff}	the effective temperature of object, defined as the temperature of a black body that would emit the same total amount of electromagnetic radiation
AU	astronomical unit, approximately equivalent to the distance between the Earth to the Sun; defined to be $149,597,870.7$ km
as	arcsecond, equivalent to $1/3600$th of a degree (standard metric prefixes apply)
pc	parsec, defined as the distance at which 1 *AU* subtends an angle of 1 *as*; approximately equivalent to 3.262 light years (standard metric prefixes apply)

1. PROLOGUE

1.1 Introduction

White dwarfs are understood as the final evolutionary step of a star whose mass is insufficient to become a neutron star or a black hole. After a low-to-medium mass main sequence star reaches the end of its hydrogen-fusing period, it will expand into a red giant, during which it fuses helium to carbon and oxygen. These giants will have insufficient mass to produce core temperatures $T_{\text{core}} \gtrsim 10^9$ K, hot enough to fuse carbon, and so an inert mass of carbon and oxygen will build up at its center. Soon after, such a star will shed its outer layers and form a planetary nebula. It will then leave behind a core, the remnant white dwarf. Thus, usually these white dwarfs remnants are composed of carbon and oxygen [4], and are only 0.008-0.02 $R_\odot$ [5]. Due to the fact that white dwarfs originate from low-to-medium mass main sequence stars, over 97% of stars in the Milky Way will end their lives as white dwarfs [6]. This can also reflected in the local density of white dwarfs, as discussed in [7]. Since a white dwarf forms from the core of a main sequences star, it initially radiates at a very high temperature, but will gradually cool as it radiates its energy away, since it no longer fuses any elements as a source of energy. This implies that a white dwarf will initially radiate with a high color temperature, but will lessen in magnitude and redden with time [8]. Over the course of a very long interval of time, the white dwarf will begin to crystallize and no longer emit any measurable amount of radiation, becoming a cold black dwarf. However, the length of this process is theorized to take loner than the current age of the universe $\tau_{\text{universe}} \simeq 13.8$ Gyr, and thus no black dwarfs are thought to exist [9], [10].

Due to their abnormal properties, white dwarfs occupy a strip at the bottom of HR-space, that is $(B-V, M_V)$ space, or equivalently $(T_{\text{eff}}, L/L_\odot)$ space, off the main sequence. They are to not be confused with other objects at the low-mass end of the main sequence, such as hydrogen-fusing M-dwarfs, whose cores are still supported by thermal pressure, unlike white dwarfs [11]. Although most are thought to be composed of carbon and oxygen, spectroscopy of their emitted

light indicates that white dwarfs retain atmospheres which are composed almost entirely of either hydrogen or helium. It is thought that this is due to the high surface gravity separating the atmosphere such that heavy elements sink below and the lighter ones, such as hydrogen and helium, float to the top [12]. Although these top layers are very thin, they are most responsible in determining the thermal and spectral evolution of the white dwarf [6]. In the Bédard cooling sequences that we make use of in our analysis, the theoretical atmospheric models can be approximated as pure Hydrogen or pure Helium due to this phenomena [13].

If a population of white dwarfs, along with main-sequence stars and other stellar objects, are formed from the same giant molecular cloud, then they can be considered part of the same open cluster. These objects follow distinct evolutionary sequences and are fundamentally related to one another, sharing many stellar parameters. Objects in an open cluster are loosely bound by mutual gravitational attraction and can become disrupted by close encounters with other clusters as they orbit the galactic center, making them a significant influence on spiral structure. In general, they survive for a few hundred million years, however more massive clusters can survive for a few billion years, allowing for the existence of open clusters composed mostly of white dwarfs [14].

1.2 Literature Review

The morphology and evolution of the local spiral structure of the Milky Way is a subject that has been debated for many decades. Once Hubble explored the M33 galaxy [15], it was postulated that the Milky Way is also a spiral galaxy. However, since the Sun is so deeply embedded in the galactic disk, it is impossible to obtain a comprehensive picture of the Milky Way in its entirety. Internal and external influences such as the dark matter halo, satellite galaxies, and open clusters, complicate it further and make it difficult to determine its exact evolution. Recent research has proven insightful, such as the analysis of substructure and morphology from [16] or the investigation of spiral tracers in [17]. However, we wish to focus on the usage of open clusters as a good tracer of the local spiral structure. The utilization of open clusters for this purpose in the literature is very thorough and thus any review in this paper would be far from comprehensive, so we refer the reader to [18]. One of the most unique advantages of utilizing open clusters as compared to

other good tracers (such as high-mass star formation region masers or massive OB stars) is the range of ages open clusters span. We thus turn our attention to white dwarfs, some of the oldest known stellar objects [9].

For any substantial investigation of the local spiral structure utilizing ancient open clusters as a tracer, a comprehensive list of white dwarf open clusters is needed. Some analysis is present in the literature, for instance more recently with regards to massive white dwarfs' role in young open clusters [19]. However, the most extensive library of white dwarf open clusters can be found in [20]. Throughout out this paper, we make use of the catalogue from [21], the largest and most comprehensive catalogue of known white dwarfs, comprising of $\sim 350\,000$ high-confidence white dwarfs.

1.3 Motivation and Synopsis

As discussed in the previous section §1.2, the primary motivation for this paper is the utilization of white dwarf open clusters as a probe for the local spiral structure of the Milky Way. Any additional clusters to the literature have the potential to provide insight concerning this topic. Open clusters can have a number of peculiar properties, but one of the most important for the investigation of the spiral structure is its position in velocity space. In particular, a cluster with abnormal positioning relative to other stellar objects can be insightful in tracing the history of spiral arms. We therefore investigate and propose the existence of a white dwarf open cluster with atypical proper motions, with 11 apparent members and an estimated cooling age (that is, the age since most of these objects have left the main sequence by stripping their outer layers and become white dwarf remnants) of 2.2(1.0) Gyr.

Recent large-scale published surveys make this analysis possible. Most significantly, the ESA's *Gaia EDR3* [1] and the Dark Energy Survey *DES Y6 Gold Release* [2]. *Gaia EDR3* is the early public installment of the third data release of the European Space Agency's *Gaia* space telescope, launched in 2013. This survey contains astrometry and photometry for 1.8 billion sources of $10 \lesssim G \lesssim 21$, the vast majority of which possess five-parameter astrometric solutions, that is $(\alpha, \delta, \varpi, \mu_\alpha, \mu_\delta)$ solutions. It is the successor to *Gaia's* second full data release, *Gaia DR2*, and

represents a significant advancement in data quality, with particular attention to an increase in parallax precision by 30% and a doubling in proper motion precisions. Additionally, systemic errors in the astrometry are suppressed by $30-40\%$ for the parallaxes and by a factor ~ 2.5 for the proper motions. It is because of this significant increase in astrometric precision and accuracy, that data from *Gaia EDR3* forms the basis of the astrometry used in this paper. *DES Y6 Gold Release* is the sixth year internal data release of the Dark Energy Survey, where the "gold" is indicative a highly refined and clean dataset. The survey utilizes *DECam* [22], mounted on the Blanco 4m telescope at Cerro Tololo Inter-American Observatory in Chile, and observes $\sim 5000\,\mathrm{deg}^2$ of the southern sky, using a $grizY$ photometric system, similar to that of the Sloan Digital Sky Survey *SDSS* [3], see Appendix 4.2. The primary goal of the Dark Energy Survey is to study the origin of cosmic acceleration and nature of dark matter, however this unprecedented survey dataset can be used in a more general context. We take advantage of its highly precise astrometry (absolute photometric uncertainties are $14, 4, 2, 15, 32\,\mathrm{mmag}$ for the $grizY$ bands, respectively), and use the dataset as the photometric basis of our sample.

§2 is dedicated to discussing the construction of our sample of 20 white dwarfs, of which we derive ages for later on. This section is divided into the following subsections: §2.1 discusses our queries of the *Gaia EDR3* and *DES Y6 Gold Release* datasets, §2.2 discusses the various quality constraints and corrections necessary to properly analyze the data, and §2.3 and §2.4 constrain the data further by making selections in color space and proper motion space, respectively, to isolate for potential members of our proposed open cluster. §3 is dedicated to discussing the derivation of ages of our sample, and the subsequent estimated age and membership of the proposed open cluster. This section is divided into the following subsections: §3.1 introduces the "Fusillo catalogue" and discusses the various stellar parameters of our sample aqurired from said catalogue, §3.2 introduces the Bédard cooling sequences and the methodology for estimated cooling ages for these objects, §3.3 discusses the estimated ages and the methodology for estimating the age of the open cluster as well as which objects can be considered as candidate members, and finally §3.4 discusses said candidate members as well as formally highlighting the estimated cooling age of this proposed

open cluster. Lastly, §4 is dedicated to discussing our findings as well as ways to improve our work, and steps that can be taken to further this investigation. This section is divided into the following subsections: §4.1 summarizes the methodology and findings of this paper as well as providing a concise account of all data used and calculated in this paper, and §4.2 discusses the various ways to improve on our investigation as well as how this data can be used for future analysis regarding white dwarf open clusters or probing of the Milky Way local spiral structure.

2. SAMPLE CONSTRUCTION

2.1 Initial Queries

As stated previously, we wish to construct a very clean sample of high proper motion white dwarfs on the order of $10^1 - 10^3$ objects, from which we can constrain in various parameter spaces to identify a closely related population of objects with abnormal velocities, potentially originating from the same source. Our sample is based in astrometry from the Gaia Early Data Release 3 so we start by querying for objects with a proper motion $\mu > 150$ mas/yr. We avoid implementing any parallax uncertainty cutoffs, as is common, for the time being. Instead we first use the information presented in [23] to correct for systematic errors from the instrument and data processing methods, then cut for parallax uncertainties later. Our query to the *Gaia Archive* (`https://gea.esac.esa.int/archive/`) is presented in Appendix 4.2. Our sample is also based in photometry from the Dark Energy Survey Year 6 Data Release (specifically the Year 6 Gold Data Release which constitutes a much cleaner version of the standard data release as well as additional parameters from supplementary data processing). We then perform a two dimensional positional cross-match between these two data sets with a maximum angular separation of 1 mas, which then returns a data set of 1,251 objects.

At this point, we note that no constraints have been implemented on this data set with regards to spectral type or distance modulus, and thus the data set so far constitutes a variety of different stellar objects with no reason for any apparent correlation or relation between them. Furthermore, while the *Gaia* footprint comprises the entire sky, the *DES* footprint does not, and therefore cannot be considered complete. The next few paragraphs outline the various constraints and data processing necessary before any subsample of white dwarfs can be determined.

2.2 Data Processing

As stated previously, due to systemic errors caused by imperfections in the instrument and data processing methods, published parallaxes from *Gaia*, especially for fainter objects, are

not in general absolute. For instance, the parallax solution with respect to certain variations of the basic angle between the directions of *Gaia's* two telescopes is degenerate [24]. Therefore, a "zero-point" offset function $Z_i(\mathbf{x})$ for each object is necessary to offset the published parallaxes to absolute parallaxes. We follow the procedure discussed in [23], which constructs a function based on *Gaia* G-band magnitude, pseudocolor ν_{eff}, and ecliptic latitude β; $Z_i(x) = Z_i(G, \nu_{\text{eff}}, \beta)$ where $i = 5, 6$ based on whether the object is published as a five-parameter or six-parameter solution. This function is valid for objects with $6 < G < 21$, and as a result, we constrain the data set to objects inside this interval. Nonetheless, the mean value of the zero-point offset functions for all objects $\overline{Z_i}(\mathbf{x}) = \varpi_{i,\text{published}} - \varpi_{i,\text{absolute}} \simeq 0.02$.

In order to properly analyze the photometry of this sample, we need adopt a convenient photometric system the allows for even comparisons between data. For this paper, we adopt the *SDSS* $ugriz$ photometric system [3]. The equations used to transform between photometric systems can be found in Appendix 4.2. As stated previously, with the majority of analysis in this paper, any photometric data will have originated from the *DES* Year 6 Data Release, which has already been dereddened. For any analysis of photometry from *Gaia*, we refer to the 3D extinction maps presented in [25] and correction functions presented in [26]

2.3 Selection in Color Space

We are now ready to analyze distance-independent color space to perform our sample selection. To do so, we compare this data set with the main-sequence isochrones presented in [27]. An isochrone is a photometric curve representing a population of stars with the same age but varying masses [28], and can be used to date open clusters because their members all have roughly the same age [29]. In this paper, we use them to verify whether or not our sample of stars constitutes an open cluster. However, in order to properly compare an isochrone with our sample on an HR Diagram, the distance to this supposed open cluster must be known a priori. Since we have yet to determine which objects would be contained in this family, we cannot analyze the isochrones on an HR Diagram. We therefore look at color space, which is intrinsically distance independent.

Though, isochrones are purposefully designed to be analyzed in HR-space, we are thus

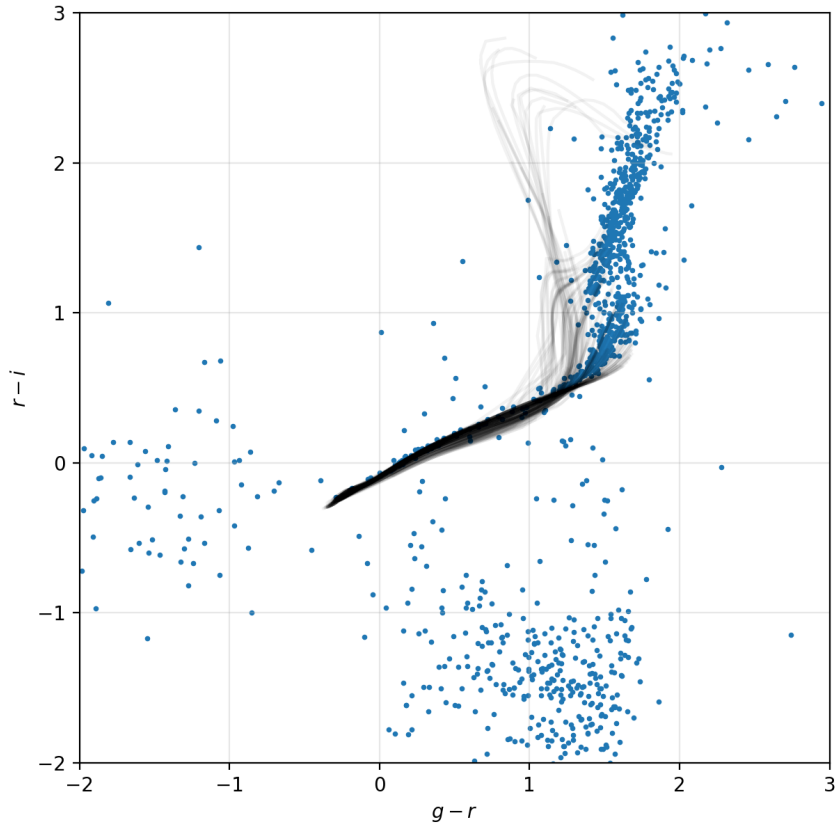

Figure 2.1: Full sample of 1 247 objects (blue) alongside a random selection of 137 isochrones (black lines, [27]) plotted in $(g-r, r-i)$ color space.

utilizing the tool that is “the isochrone" outside of its intended purpose. In HR-space, objects that lie along a single isochrone are of varying mass (and thus different magnitude and color) but similar age and initial composition. Hence, the ability to date clusters. In color space, the isochrone plays a slightly different role since a third magnitude is introduced. Here, the previous relation between parameters ceases to be the case. That is, objects from the same open cluster do not necessarily lie on the same isochrone. Despite this, we can still hypothesize the existence of a closely-related group of stars by inspecting a small portion of the isochrone, and functionally “approximate" a color-color relation between objects of a supposed open cluster.

We take a random sample of 137 main-sequence isochrones as well as our sample as it currently stands and and plot them in $(g-r, r-i)$ color space, Figure 2.1. An unusual pattern

emerges in the vicinity of $1 < (g-r) < 2$, $0.5 < (r-i) < 2.5$, as well as a large number of extraneous objects in the low $(r-i)$ and low $(g-r)$ regimes. For the time being, we disregard these extraneous objects, as well as the spur from isochrones constituting the majority of these objects. A future investigation of these objects could prove useful. However, we instead select the 56 objects that lie in and around the dense linear cluster of isochrones from $-0.3 < (g-r) < 1.2$, $-0.3 < (r-i) < 0.4$. These objects are most likely to originate from the same source, and so we continue our sample construction with these objects.

At this point, we should acknowledge how from this selection in a CCD, near exclusively white dwarfs are selected. The mechanism for this process is unknown at the moment and any investigation is scarce throughout the literature. Further analysis might prove useful. However, we disregard this for the time being, and instead provide the reader with further reading on the interactions and characteristics of white dwarfs in color-color space: [30], [31], [32].

2.4 Selection in Proper Motion Space

We now turn out attention to proper motion, $(\mu_{\alpha*}, \mu_\delta)$ or $(\mu_{\ell*}, \mu_b)$ space, where we wish to define a subsample to analyze more closely. One of the most telling properties of an open cluster is that all objects within that cluster reside in a specific region of velocity phase space. Thus, analyzing the distribution of velocities of our sample could provide insight on the origin of the objects. However, the vast majority of the remaining 56 objects possess five-parameter astrometric solutions from *Gaia*, that is $(\alpha, \delta, \varpi, \mu_\alpha, \mu_\delta)$ are known, but v_{radial} remains unknown. Therefore, we cannot properly analyze Cartesian velocity phase space, and must settle for the slightly less illuminating proper motion, or tangential velocity, phase space.

$$v_q = 4.74 \mu \varpi \tag{Eq. 1}$$

We confine our subsample to the $(+\mu_{\ell*}, +\mu_b)$ space, as displayed in Figure 2.2b. This corresponds to a tangent velocity, calculated using Eq (Eq. 1), roughly opposite the direction of galactic spin, with velocity magnitudes comparable to the orbital speed of the Milky Way in the solar neighborhood [33], as shown in Figures 2.2a and 2.2c. However, we reiterate again that

these are two-parameter velocity solutions and thus considerable information regarding the orbital trajectories of these objects remains unknown. Nonetheless, the accuracy of these proper motion and parallax measurments from *Gaia*, as shown in Figure 2.2d, allow us to confidently constrain this subsample in proper motion phase space.

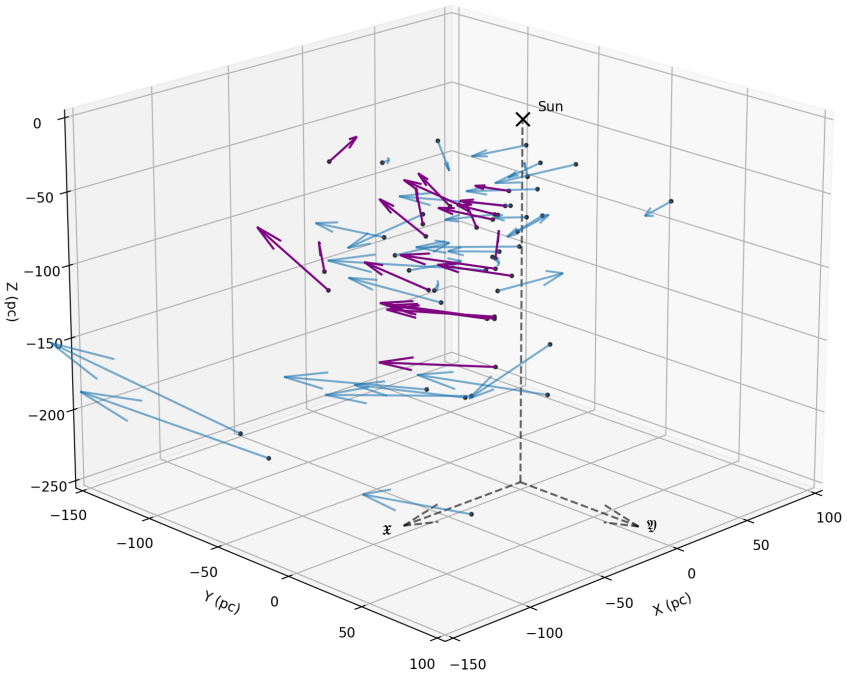

(a)

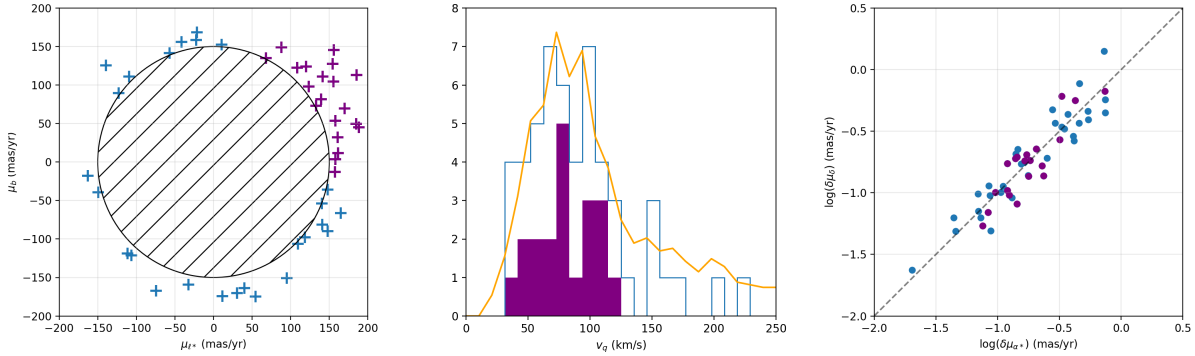

(b) (c) (d)

Figure 2.2: Sample of 56 chromatically related objects (blue) with subsample of 20 objects selected based on proper motions (purple) in: (**a**) 3D cartesian space with tangent velocity vectors $\mathbf{v}_q$ whose length is proportional to v_q ($\mathfrak{X}$ points in the direction of the galactic center and $\mathfrak{Y}$ points in the direction of galactic spin), (**b**) plotted in proper motion $(\mu_{\ell*}, \mu_b)$ space, with the hatched circle representing the region of $\mu < 150$ mas/yr, the initial proper motion cutoff from the *Gaia* query, (**c**) tangent velocity v_q distribution with a rough, scaled distribution of the 1,256 original objects in the same phase space (orange), and **d** proper motion uncertainty $(\delta\mu_{\alpha*}, \mu_\delta)$ space.

3. Age Derivation

3.1 Stellar Parameters

As stated previously, white dwarf atmospheres can be approximately modeled as purely hydrogen, purely helium, or a mixed H-He atmosphere [34]. We can then use these atmospheric models to calculate stellar parameters, most importantly mass, which then allows us to fit our objects onto theoretical cooling sequences, and thus derive an approximate age for each object. At this point, we introduce a catalogue of $\simeq 359,000$ high confidence white dwarfs from *Gaia*, from hereon referred to as the "Fusillo Catalogue" [21].

Of interest to us from the Fusillo catalogue is the probability of being a white dwarf $P_{\rm WD}$ for each object, in which methods described in [35] are employed to calculate this parameter. A sample of $\sim 22\,000$ spectroscopically confirmed white dwarfs are mapped onto HR-space using *Gaia DR2* photometry. From there, positions in this space can be used to calculate $P_{\rm WD}$ for each photometrically reliable object in *Gaia EDR3*. By construction, all 20 objects in our sample have an entry in the Fusillo catalogue, in which we use *Gaia* `source_id` to identify matches. From this, we can see that our objects all have $P_{\rm WD} > 0.98$, and can thus be classified as high-confidence white dwarfs. This can also be seen in Figure 3.1 where our objects reside clearly in the high-confidence white dwarf region in HR-space.

The methods used to calculate stellar parameters, such as effective temperature $T_{\rm eff}$, log surface gravity $\log g$, and mass M, for the Fusillo catalog are very complicated, and we thus refer the reader to §4.0 of [35]. In brief, for pure-H atmospheres, the grid from [36] is employed with Lyman α opacity from [37]. For pure-He atmospheres, the grid from [38] is used. And for mixed H-He atmospheres, a composition of H/He $= 10^{-5}$ is used, where a third grid based on calculations from [39] and [40] is employed. Mass and radius can be determined directly from the models from [13] and [41], whereas $T_{\rm eff}$ and $\log g$ can be calculated using other methods. These stellar parameters are calculated using all three model atmospheres. The non-linear least-squares

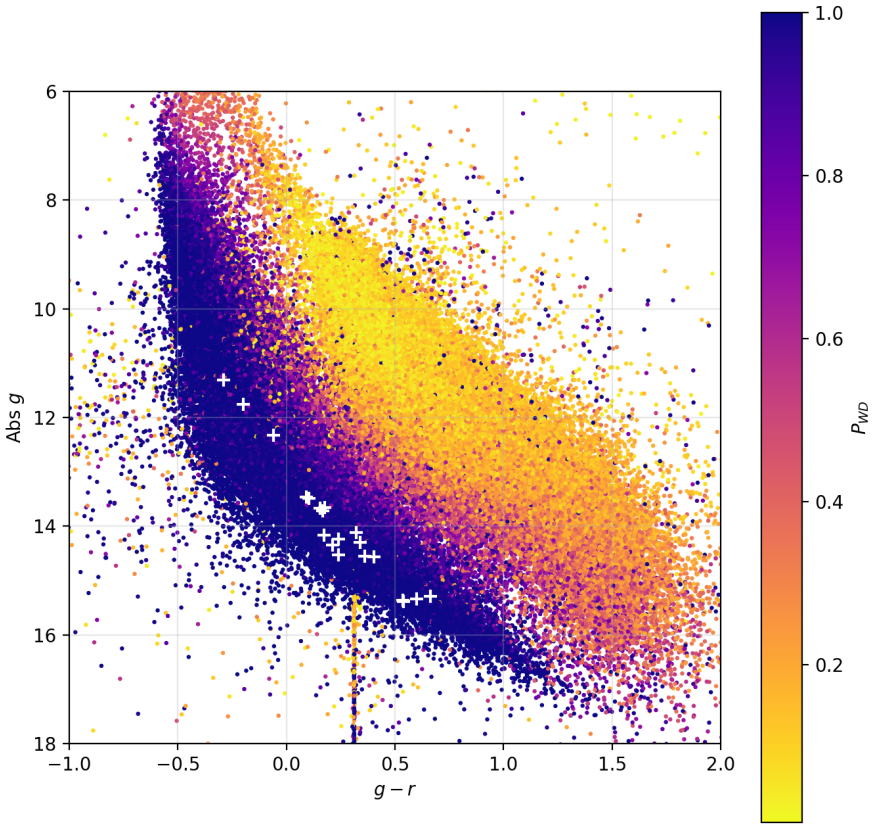

Figure 3.1: All 1 280 266 objects from the full Fusillo catalogue [21] plotted in HR $(g - r,\ G)$ space, with color scale reflecting the P_{WD} value for each object; white "+"s are the constrained sample of 20 objects as defined in §2.4.

fitting method of Levenberg-Marquardt is then applied to the models, producing a χ^2 value for each model. We then use this χ^2 value to select an atmospheric model for each object in our sample that best fits. This results in 12 objects modeled with pure-H atmospheres, 8 objects with pure-He, and zero objects with mixed H-He atmospheres.

3.2 Cooling Sequences

We are now in a position to derive ages for each of our objects from *DES* photometry and the stellar parameters provided in the Fusillo catalogue. At this point, we introduce the Bédard cooling sequences, described in [13]. These theoretical cooling sequences are the successor to the "Montreal Sequences", as described in [6], and allow for analysis of hotter white dwarfs ($T_{\mathrm{eff}} \gtrsim 30,000$ K). For a given mass M such that $0.2\,M_{\odot} \leq M \leq 1.3\,M_{\odot}$, there exists a contour in HR-

space that can be parameterized by age. That is, if the location of an object along this contour is known, the age of the object can be estimated.

The Bédard cooling sequences represent the culmination of much theoretical and computational research, and are thus integral in improving understanding of the spectral evolution of hot white dwarfs. The derivation and model-building are far too complicated to discuss in this paper, and we hence refer the reader to §3.2 of [13] for further discussion of the evolutionary cooling sequences. We employ two model grids for our objects, corresponding to a pure-H atmosphere and pure-He atmosphere. As discussed previously in §3.1, we approximate each of our objects as having pure-H atmospheres or pure-He atmosphere based on the findings of [21]. We reiterate that these findings are based on *Gaia* photometry and thus a similar analysis utilizing *DES* photometry may prove to yield different results. We place our objects in HR-space alongside their corresponding pure-H or pure-He cooling sequences, as seen in Figure 3.2. Our objects are placed in HR-space using *DES* photometry, but still employing the *SDSS* photometric system. We then choose the closet cooling sequences in increments of $0.1\,M_{\odot}$ based on the masses derived in the Fusillo catalogue and the positions of our objects in HR-space. Once the contour for a given object is known, we find the corresponding age, using linear approximations for positions between grid points.

3.3 Age Results

Table 3.1 displays the estimated cooling ages of our sample, as described in §2, as well as the rest of the most notable columns used throughout this paper. The astrometry and photometry represent a very clean sample with all objects flagged as high-confidence white dwarfs; all objects have $\delta\varpi/\varpi < 0.1$, $\delta\mu/\mu < 0.1$, $\delta g/g < 0.1$, and $\delta r/r < 0.1$. We wish to reiterate the large uncertainties associated with T_{eff} and M; uncertainties are on the order of $\sim 10^2$ K and $\sim 10^{-1}\,M_{\odot}$, respectively. The exact uncertainties can be publicly downloaded from (`https://warwick.ac.uk/fac/sci/physics/research/astro/research/catalogues/`), see [21] for details.

Estimating uncertainties for ages is difficult, given the multitude of parameters used to find

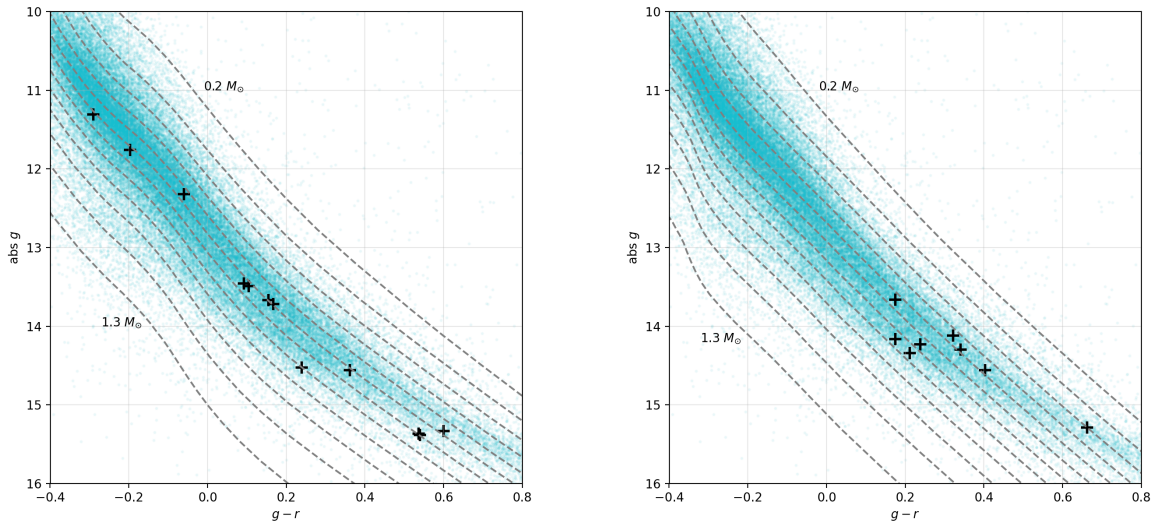

(a) (b)

Figure 3.2: Pure-H atmosphere and pure-He atmosphere (a and b, respectively) cooling sequences plotted on HR-space (gray dashed lines). Cooling sequences are displayed in intervals of $0.1\,M_\odot$, ranging from $0.2\,M_\odot$ on the right to $1.3\,M_\odot$ on the left. Objects in the Fusillo catalogue with $P_{\rm WD} > 0.95$ are also displayed (blue). Black "+"s are objects from our constrained sample as described in §2.4. Objects are only plotted with their corresponding atmospheric model.

the results. While the astrometry and photometry provide a very accurate and precise base of measurments, the large uncertainties in effective temperature and mass, as well as the approximate theoretical atmospheric models, make any assured conclusions challenging. As stated previously, most uncertainties in the columns are on the order of $\sim 10\%$, however some are upwards of 30%, such as the uncertainty in mass for *Gaia EDR3* `5170247786582669952`, $\delta M/M \simeq 0.34$. We therefore estimate the uncertainties for each cooling age estimate to be on the order of $\delta\tau \simeq 1.0$ Gyr.

3.4 Candidate Open Cluster Members

We are now in a position to make the finally constraint on which objects are candidates for member of a hypothetical new open cluster, this time by an estimated cooling age τ. Figure 3.3 displays the last column in Table 3.1, including uncertainties. From here, we can estimate a cooling age of the cluster and determine which objects should be classified as candidate open

Table 3.1: Our sample of 20 objects, as described in §2.3 and §2.4, with our derived ages, as discussed in §3.2. Uncertainties can be found in the Fusillo catalogue [21] and are available upon request. All ages have an uncertainty of 1.0 Gyr.

Gaia `source_id`	d (pc)	μ ($\frac{\text{mas}}{\text{yr}}$)	g_{abs}	$g-r$	T_{eff} (K)	M ($M_\odot$)	τ (Gyr)
4863793139509359 36	154.057	151.200	14.53	0.2395	6142	0.729	4.4
2451440648201537664	157.633	151.569	11.31	-0.2908	12815	0.540	0.3
5043539001446104576	130.375	157.354	14.30	0.3407	6227	0.589	2.4
2885007151372669440	107.868	157.707	14.16	0.1748	6443	0.646	2.7
5090839922953562752	136.669	157.900	13.72	0.1670	6809	0.576	1.6
2512123111550915968	45.231	161.283	13.49	0.1053	7839	0.729	1.6
2351410413201636224	102.425	161.562	14.34	0.2115	6247	0.660	3.0
2518822538978075904	61.237	163.708	12.32	-0.0598	9501	0.576	6.7
5170247786582669952	115.114	163.996	15.38	0.5405	5505	0.790	6.4
5028471775135109760	97.521	166.509	14.56	0.3622	6177	0.705	3.5
5058944087064090112	92.194	172.462	14.23	0.2388	6646	0.716	2.8
5037961629930644608	67.334	172.911	14.56	0.4030	5846	0.569	2.7
2467261246135974400	54.178	179.706	15.33	0.5997	5415	0.707	5.8
5047024693824366720	90.595	183.543	14.12	0.3218	6035	0.473	1.9
2477828308798036352	122.178	187.197	13.46	0.0928	7882	0.718	1.6
2354251727341074816	127.779	191.094	13.66	0.1745	7322	0.641	1.7
5020128543464883840	77.143	193.448	13.67	0.1553	7473	0.712	1.6
5057830865900543232	69.730	200.004	15.37	0.5372	5419	0.747	6.2
5167411493260087040	60.988	213.361	15.29	0.6623	5127	0.522	4.9
2512346415490500864	93.547	217.102	11.76	-0.1973	11992	0.650	0.4

cluster members.

We therefore estimate an open cluster cooling age of $\tau_{\text{cluster}} = 2.2(1.0)$ Gyr. We then select objects whose estimated age falls within this value, which signifies 11 different objects, as listed in Table 3.2, along with corresponding tangent velocities. These objects represent our final sample, and the most apparent candidate members of this possible new open cluster.

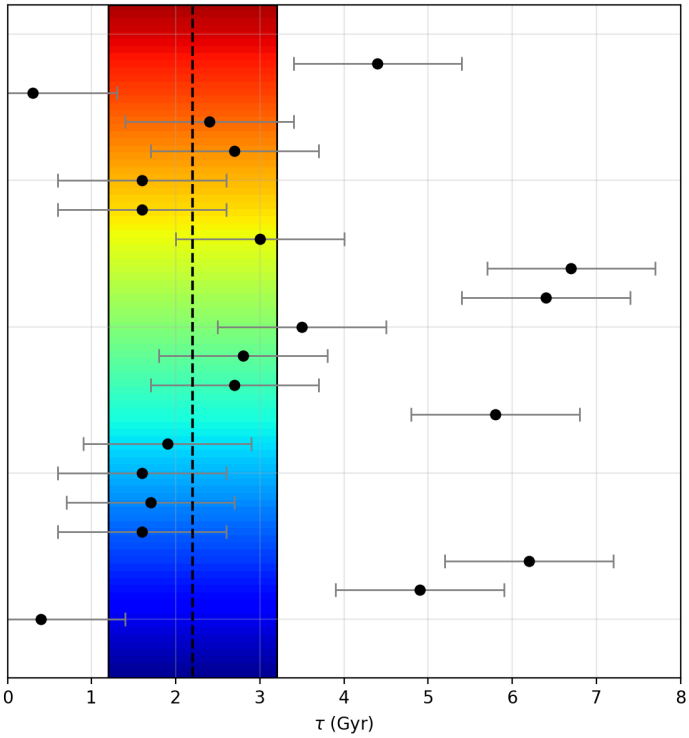

Figure 3.3: Ages of all 20 objects of our sample plotted in order as listed in Table 3.1 (black). Uncertainties are represented by gray error bars. Our estimated age of the candidate open cluster is displayed with a black dashed line, with uncertainty bounds displayed with solid black lines. The potential age of cluster is shaded in rainbow.

Table 3.2: Candidate open cluster members with tangent velocity v_q as well as estimated cooling age.

Gaia EDR3 `source_id`	v_q (km/s)	Age (Gyr)
5043539001446104576	97.251	2.4
2885007151372669440	80.643	2.7
5090839922953562752	102.299	1.6
2512123111550915968	34.581	1.6
2351410413201636224	78.445	3.0
5058944087064090112	75.374	2.8
5037961629930644608	55.192	2.7
5047024693824366720	78.825	1.9
2477828308798036352	108.421	1.6
2354251727341074816	115.751	1.7
5020128543464883840	70.743	1.6

4. EPILOGUE

4.1 Summary

We have provided moderate evidence for the potential of a new open cluster, one with irregular tangent velocities, hinting at the possibility of an abnormal origin. We have determined 11 objects in which we deem candidate cluster members. All objects are white dwarfs with masses $\sim 0.5 - 0.8\ M_{\odot}$ and cooling ages $\sim 1.2 - 3.2$ Gyr, thereby also dating the open cluster. These objects contain excellent astrometry from *Gaia* and photometry from *DES*. All of these objects have entries in *Simbad* (`http://simbad.u-strasbg.fr/simbad/`), and are only logged as being identified in *Gaia* and the Fusillo catalogue [21]. Therefore, this cluster, for it to be genuine, will be a new discovery.

To summarize our methodology, we first queried for high proper motion objects in *Gaia EDR3×DES Y6*. We then used the Dartmouth stellar isochrones [27] to constrain our sample to objects highly clustered along a linear section of the isochrones in color space, where almost exclusively white dwarfs arose. From there, we further constrained the sample in proper motion space. At this point, we possessed a clean sample of 20 astrometrically and photometrically related objects. We then used data from the Fusillo catalogue [21] and the Bédard theoretical cooling sequences [13] to derive rough cooling ages for all white dwarfs. Finally, we constrained our sample to 11 objects whose cooling ages corresponded with the estimated age of the open cluster, $\tau_{\text{cluster}} = 2.2(1.0)$ Gyr. Tables 3.1 & 3.2 are the culmination of this paper and thus provide another brief overview of the methodology and purpose of this paper.

Once again, a list of the columns and the origin of their data for Table 3.1 is as follows. Distance $d = \varpi^{-1}$ and proper motion $\mu = (\mu_{\alpha*}^2 + \mu_{\delta}^2)^{1/2}$ are directly from *Gaia EDR3*. Absolute G-band mean magnitude g_{abs} and color $g-r$ photometry is taken directly from *DES Y6 Gold* and is displayed in the *SDSS/UKIDSS* $grizY$ photometric system. Type of atmospheric model, effective temperature T_{eff}, and mass M are obtained from the Fusillo catalogue [21]. Finally, cooling age τ

was estimated, as described in §3.2-3.3.

Appendix 4.2 lists the *Gaia Archive* and *DES Access* queries used to initiate our sample, as described in §2.1. Appendix 4.2 lists the various equations used in this paper to transform between photometric systems, most importantly between *DES* $grizy$ and *SDSS/UKIDSS* $grizY$.

4.2 Moving Forward

There are a number of ways to improve the results of this paper, that is to provide stronger evidence for the existence of this supposed new open cluster and estimate a more precise age of said cluster. Improvements can be made with regards to almost every aspect of the analysis presented, most significantly via the data, theory, and methodology. We discuss some of these methods of improvement in the following.

Firstly, with regards to data. Obviously, the instruments themselves will always have the capacity (and necessity) to improve with precision and accuracy. *Gaia DR3* and *DR4*, planned for release Q2 2022 and 2025, respectively, will mark further improvements in astrometry. Additional sources of photometric information such as the upcoming *Vera C. Rubin Observatory* (`https://www.lsst.org/`) could supplement *DES* photometry, and could allow for more accurate positioning of objects in HR-space. Most significantly however, the parameters obtained from the Fusillo catalogue used to estimate cooling ages for our sample, effective temperature T_{eff} and mass M, were calculated using *SDSS* photometry. It is well known that *SDSS* photometry is vastly inferior when compared to *DES*, for instance, in almost every metric. Of course, one could bypass this obstacle by replicating the methods outlined in [21] using *DES* photometry instead of *SDSS*. Although difficult to estimate the possibility of measurements in the near future, line of sight velocities of these objects are crucial in understanding the full picture of their positions in velocity space. And by extension, our understanding of the potential new open cluster remains hindered by this lack of data. Additionally, more rigorous queries have the potential to provide more compelling evidence, as a cleaner and more reliable sample might be constructed.

Secondly, although [13] represents a large leap in the understanding of white dwarf cooling sequences, they still remain poorly understood. Therefore, more accurate theoretical models for

the structure and evolution of white dwarfs, particularly hot white dwarfs, would prove useful in analyses such as the one presented in this paper. Stellar parameters in the Fusillo catalogue also rely on the Bédard cooling sequences, and so any marginal improvement in precision or accuracy of the white dwarf cooling sequences has the potential to vastly improve our final results.

Lastly, significant improvements can be made to the methodology of this paper to produce more certain results. As said previously, replicating the process in [21] to derive stellar parameters using *DES* photometry instead of *SDSS* photometry could prove to yield smaller uncertainties and thus more precise stellar parameters. A deeper understanding of the stellar isochrones in color space would also likely lead to more accurate results, as their particular behavior is poorly understood and scarce in the literature. Finally, more rigorous fitting techniques when constraining data and estimating ages are required to reliably assess the validity of these candidate open cluster members.

REFERENCES

[1] Gaia Collaboration, "Gaia Early Data Release 3. Summary of the contents and survey properties," *Astronomy and Astrophyiscs*, vol. 649, p. A1, May 2021.

[2] DES Collaboration, "Dark Energy Survey Year 1 Results: The Photometric Data Set for Cosmology," *The Astrophysical Journal*, vol. 235, p. 33, Apr. 2018.

[3] SDSS Collaboration, "The Seventeenth Data Release of the Sloan Digital Sky Surveys: Complete Release of MaNGA, MaStar, and APOGEE-2 Data," *The Astrophysical Journal*, vol. 259, p. 35, Apr. 2022.

[4] K. Werner, N. J. Hammer, T. Nagel, T. Rauch, and S. Dreizler, "On Possible Oxygen/Neon White Dwarfs: H1504+65 and the White Dwarf Donors in Ultracompact X-ray Binaries," in *14th European Workshop on White Dwarfs* (D. Koester and S. Moehler, eds.), vol. 334 of *Astronomical Society of the Pacific Conference Series*, p. 165, July 2005.

[5] H. L. Shipman, "Masses and radii of white-dwarf stars. III. Results for 110 hydrogen-rich and 28 helium-rich stars.," *The Astrophysical Journal*, vol. 228, pp. 240–256, Feb. 1979.

[6] G. Fontaine, P. Brassard, and P. Bergeron, "The Potential of White Dwarf Cosmochronology," *Publications of the Astronomical Society of the Pacific*, vol. 113, pp. 409–435, Apr. 2001.

[7] J. B. Holberg, T. D. Oswalt, and E. M. Sion, "A Determination of the Local Density of White Dwarf Stars," *The Astrophysical Journal*, vol. 571, pp. 512–518, May 2002.

[8] J. B. Holberg, "How Degenerate Stars Came to be Known as White Dwarfs," in *American Astronomical Society Meeting Abstracts*, vol. 207 of *American Astronomical Society Meeting Abstracts*, p. 205.01, Dec. 2005.

[9] A. Heger, C. L. Fryer, S. E. Woosley, N. Langer, and D. H. Hartmann, "How Massive Single Stars End Their Life," *The Astrophysical Journal*, vol. 591, pp. 288–300, July 2003.

[10] D. N. Spergel, R. Bean, O. Doré, M. R. Nolta, C. L. Bennett, J. Dunkley, G. Hinshaw, N. Jarosik, E. Komatsu, L. Page, H. V. Peiris, L. Verde, M. Halpern, R. S. Hill, A. Kogut, M. Limon, S. S. Meyer, N. Odegard, G. S. Tucker, J. L. Weiland, E. Wollack, and E. L.

Wright, "Three-Year Wilkinson Microwave Anisotropy Probe (WMAP) Observations: Implications for Cosmology," *The Astrophysical Journal Supplemental Series*, vol. 170, pp. 377–408, June 2007.

[11] G. Chabrier and I. Baraffe, "Theory of Low-Mass Stars and Substellar Objects," *Annual Review of Astronomy and Astrophysics*, vol. 38, pp. 337–377, Jan. 2000.

[12] E. Schatzman, "Théorie du débit d'énergie des naines blanches," *Annales d'Astrophysique*, vol. 8, p. 143, Jan. 1945.

[13] A. Bédard, P. Bergeron, P. Brassard, and G. Fontaine, "On the Spectral Evolution of Hot White Dwarf Stars. I. A Detailed Model Atmosphere Analysis of Hot White Dwarfs from SDSS DR12," *The Astrophysical Journal*, vol. 901, p. 93, Oct. 2020.

[14] C. Payne-Gaposchkin, *Stars and clusters*. 1979.

[15] E. P. Hubble, "A spiral nebula as a stellar system: Messier 33.," *The Astrophysical Journal*, vol. 63, pp. 236–274, May 1926.

[16] T. Antoja, A. Helmi, M. Romero-Gómez, D. Katz, C. Babusiaux, R. Drimmel, D. W. Evans, F. Figueras, E. Poggio, C. Reylé, A. C. Robin, G. Seabroke, and C. Soubiran, "A dynamically young and perturbed Milky Way disk," *Nature*, vol. 561, pp. 360–362, Sept. 2018.

[17] L. G. Hou and J. L. Han, "The observed spiral structure of the Milky Way," *Astronomy and Astrophyiscs*, vol. 569, p. A125, Sept. 2014.

[18] C. J. Hao, Y. Xu, L. G. Hou, S. B. Bian, J. J. Li, Z. Y. Wu, Z. H. He, Y. J. Li, and D. J. Liu, "Evolution of the local spiral structure of the Milky Way revealed by open clusters," *Astronomy and Astrophyiscs*, vol. 652, p. A102, Aug. 2021.

[19] H. B. Richer, I. Caiazzo, H. Du, S. Grondin, J. Hegarty, J. Heyl, R. Kerr, D. R. Miller, and S. Thiele, "Massive White Dwarfs in Young Star Clusters," *The Astrophysical Journal*, vol. 912, p. 165, May 2021.

[20] M. Prišegen, M. Piecka, N. Faltová, M. Kajan, and E. Paunzen, "White dwarf-open cluster associations based on Gaia DR2," *Astronomy and Astrophyiscs*, vol. 645, p. A13, Jan. 2021.

[21] N. P. Gentile Fusillo, P. E. Tremblay, E. Cukanovaite, A. Vorontseva, R. Lallement, M. Hollands, B. T. Gänsicke, K. B. Burdge, J. McCleery, and S. Jordan, "A catalogue of white dwarfs

in Gaia EDR3," *Monthy Notices of the Royal Astronomical Society*, vol. 508, pp. 3877–3896, Dec. 2021.

[22] DES Collaboration, "The Dark Energy Camera," *The Astronomical Journal*, vol. 150, p. 150, Nov. 2015.

[23] L. Lindegren, U. Bastian, M. Biermann, A. Bombrun, A. de Torres, E. Gerlach, R. Geyer, J. Hernández, T. Hilger, D. Hobbs, S. A. Klioner, U. Lammers, P. J. McMillan, M. Ramos-Lerate, H. Steidelmüller, C. A. Stephenson, and F. van Leeuwen, "Gaia Early Data Release 3. Parallax bias versus magnitude, colour, and position," *Astronomy and Astrophyiscs*, vol. 649, p. A4, May 2021.

[24] A. G. Butkevich, S. A. Klioner, L. Lindegren, D. Hobbs, and F. van Leeuwen, "Impact of basic angle variations on the parallax zero point for a scanning astrometric satellite," *The Astrophysical Journal*, vol. 603, p. A45, July 2017.

[25] G. M. Green, E. Schlafly, C. Zucker, J. S. Speagle, and D. Finkbeiner, "A 3D Dust Map Based on Gaia, Pan-STARRS 1, and 2MASS," *The Astrophysical Journal*, vol. 887, p. 93, Dec. 2019.

[26] Gaia Collaboration, "Gaia Data Release 2. Observational Hertzsprung-Russell diagrams," *Astronomy and Astrophyiscs*, vol. 616, p. A10, Aug. 2018.

[27] A. Dotter, B. Chaboyer, D. Jevremović, V. Kostov, E. Baron, and J. W. Ferguson, "The Dartmouth Stellar Evolution Database," *The Astrophysical Journal*, vol. 178, pp. 89–101, Sept. 2008.

[28] R. Kippenhahn, A. Weigert, and A. Weiss, *Stellar Structure and Evolution*. 2012.

[29] A. Frebel, *Searching for the Oldest Stars: Ancient Relics from the Early Universe*. Princeton University Press, 2015.

[30] R. Szczerba, N. Siódmiak, A. Leśniewska, A. Karska, and M. Sewiło, "Stellar evolution in the outer Galaxy," in *Journal of Physics Conference Series*, vol. 728 of *Journal of Physics Conference Series*, p. 042004, July 2016.

[31] P. D. Dobbie, A. Day-Jones, K. A. Williams, S. L. Casewell, M. R. Burleigh, N. Lodieu, Q. A. Parker, and R. Baxter, "Further investigation of white dwarfs in the open clusters NGC 2287 and NGC 3532," *Monthy Notices of the Royal Astronomical Society*, vol. 423, pp. 2815–2828, July 2012.

[32] R. Raddi, S. Catalán, B. T. Gänsicke, J. J. Hermes, R. Napiwotzki, D. Koester, P. E. Tremblay, G. Barentsen, H. J. Farnhill, M. Mohr-Smith, J. E. Drew, P. J. Groot, L. Guzman-Ramirez, Q. A. Parker, D. Steeghs, and A. Zijlstra, "A search for white dwarfs in the Galactic plane: the field and the open cluster population," *Monthy Notices of the Royal Astronomical Society*, vol. 457, pp. 1988–2004, Apr. 2016.

[33] L. L. Watkins, R. P. van der Marel, S. T. Sohn, and N. W. Evans, "Evidence for an Intermediate-mass Milky Way from Gaia DR2 Halo Globular Cluster Motions," *The Astrophysical Journal*, vol. 873, p. 118, Mar. 2019.

[34] G. Fontaine and F. Wesemael, "White Dwarfs," in *Encyclopedia of Astronomy and Astrophysics* (P. Murdin, ed.), p. 1894, 2000.

[35] N. P. Gentile Fusillo, P.-E. Tremblay, B. T. Gänsicke, C. J. Manser, T. Cunningham, E. Cukanovaite, M. Hollands, T. Marsh, R. Raddi, S. Jordan, S. Toonen, S. Geier, M. Barstow, and J. D. Cummings, "A Gaia Data Release 2 catalogue of white dwarfs and a comparison with SDSS," *Monthy Notices of the Royal Astronomical Society*, vol. 482, pp. 4570–4591, Feb. 2019.

[36] P. E. Tremblay, P. Bergeron, and A. Gianninas, "An Improved Spectroscopic Analysis of DA White Dwarfs from the Sloan Digital Sky Survey Data Release 4," *The Astrophysical Journal*, vol. 730, p. 128, Apr. 2011.

[37] P. M. Kowalski and D. Saumon, "Found: The Missing Blue Opacity in Atmosphere Models of Cool Hydrogen White Dwarfs," *The Astrophysical Journal*, vol. 651, pp. L137–L140, Nov. 2006.

[38] P. Bergeron, F. Wesemael, P. Dufour, A. Beauchamp, C. Hunter, R. A. Saffer, A. Gianninas, M. T. Ruiz, M. M. Limoges, P. Dufour, G. Fontaine, and J. Liebert, "A Comprehensive Spectroscopic Analysis of DB White Dwarfs," *The Astrophysical Journal*, vol. 737, p. 28, Aug. 2011.

[39] P. E. Tremblay, J. S. Kalirai, D. R. Soderblom, M. Cignoni, and J. Cummings, "White Dwarf Cosmochronology in the Solar Neighborhood," *The Astrophysical Journal*, vol. 791, p. 92, Aug. 2014.

[40] J. McCleery, P.-E. Tremblay, N. P. Gentile Fusillo, M. A. Hollands, B. T. Gänsicke, P. Izquierdo, S. Toonen, T. Cunningham, and A. Rebassa-Mansergas, "Gaia white dwarfs within 40 pc II: the volume-limited Northern hemisphere sample," *Monthy Notices of the Royal Astronomical Society*, vol. 499, pp. 1890–1908, Dec. 2020.

[41] A. M. Serenelli, L. G. Althaus, R. D. Rohrmann, and O. G. Benvenuto, "The ages and colours of cool helium-core white dwarf stars," *Monthy Notices of the Royal Astronomical Society*, vol. 325, pp. 607–616, Aug. 2001.

[42] K. Jordi, E. K. Grebel, and K. Ammon, "Empirical color transformations between SDSS photometry and other photometric systems," *The Astrophysical Journal*, vol. 460, pp. 339–347, Dec. 2006.

APPENDIX A: Queries

The initial query from the *Gaia Archive* in which we query for a complete sample with a proper motion lower bound of 150 mas/yr is given below. The query returned $155\,951$ objects.

```
SELECT g3.* , g2.teff_val
FROM gaiaedr3.gaia_source as
g3 join gaiadr2.gaia_source as g2
ON g3.source_id = g2.source_id
WHERE g3.pm >= 150
```

The initial query from *DES Access* in which we query for a photometrically clean stellar sample is given below. The query returned $47\,108\,496$ objects.

```
SELECT *
FROM Y6_GOLD_2_0
WHERE EXT_COADD = 0 AND MAG_AUTO_G > 11
AND MAGERR_AUTO_G / MAG_AUTO_G < 0.1
AND MAGERR_AUTO_R / MAG_AUTO_R < 0.1
AND MAGERR_AUTO_I / MAG_AUTO_I < 0.1
AND MAGERR_AUTO_Z / MAG_AUTO_Z < 0.1
AND MAGERR_AUTO_Y / MAG_AUTO_Y < 0.1
```

APPENDIX B: Photometric Transformation Equations

The photometric transformation equations between the DES $grizy$ system and the SDSS/UKIDSS $grizy$ system can be found in [2], and are reiterated below (Eq. 1).

$$
\begin{aligned}
g_{\text{SDSS}} &= g_{\text{DES}} + 0.104(g-r)_{\text{DES}} - 0.01 \\
r_{\text{SDSS}} &= r_{\text{DES}} + 0.102(g-r)_{\text{DES}} - 0.02 \\
i_{\text{SDSS}} &= i_{\text{DES}} + 0.256(i-z)_{\text{DES}} - 0.02 \\
z_{\text{SDSS}} &= z_{\text{DES}} + 0.086(i-z)_{\text{DES}} - 0.01 \\
y_{\text{UKIDSS}} &= y_{\text{DES}} - 0.312(z-y)_{\text{DES}} \\
&\quad - 0.205(i-y)_{\text{DES}} - 0.829
\end{aligned}
\qquad \text{(Eq. 1)}
$$

The photometric transformation equations between the SDSS/UKIDSS $grizy$ system and the Johnston-Cousins BVR_CI_C systemcan be found in §3.1 of [42], and are reiterated below (Eq. 2).

$$
\begin{aligned}
B &= g + 0.312(g-r) + 0.219 \\
V &= g - 0.573(g-r) - 0.016 \\
R_C &= r - 0.257(r-i) + 0.152 \\
I_C &= i - 0.409(i-z) - 0.394
\end{aligned}
\qquad \text{(Eq. 2)}
$$